

Hyperspherical approach to double-electron excitation of He by fast-ion impact. II. Excitation to the $(2l3l')$ and $(3l3l')$ manifolds by proton and antiproton impact

Kengo Moribayashi, Ken-ichi Hino, and Michio Matsuzawa

*Department of Applied Physics and Chemistry,
The University of Electro-Communications,
1-5-1 Chofu-ga-oka Chofu-shi, Tokyo 182, Japan*

M. Kimura

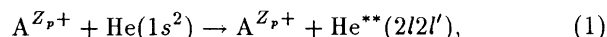
*Argonne National Laboratory, Argonne, Illinois 60439
and Department of Physics, Rice University, Houston, Texas 77251
(Received 25 November 1991)*

Double-electron excitation processes of He atoms from the ground state to the manifolds of the doubly excited $2l3l'$ and $3l3l'$ states by proton and antiproton impact have been theoretically investigated using a close-coupling method at the 1.5-MeV/u energy regime. The semiclassical impact-parameter method with a straight-line-trajectory approximation is employed to describe collision processes. Hyperspherical wave functions are adopted to take full account of strongly correlated motion of two atomic electrons in He. The difference between the cross section by proton impact and that by antiproton impact is small except for the process to the $3p3p^1S^e$ state. The reason for the small difference between $\sigma(p)$ and $\sigma(\bar{p})$ is discussed. The $^1P^o$ states are found to play an important role as intermediate ones. For the process to the doubly excited $2l3l'$ states, the $(2s3p + 3s2p)^1P^o$ state plays a crucial role. For the excitation process to the $3l3l'$ states, the ratio of the second-order process to the first-order one is larger than that in the case of the process to the $2l2l'$ and $2l3l'$ states, suggesting that the difference between the mechanism of the excitation to the $(2l, 2l')$ and $(2l, 3l')$ manifolds and that to the $(3l, 3l')$ manifold arises from the smaller overlap of the $(3l, 3l')$ wave functions with that of the ground state. It is seen that the physical interpretation of the results based on the rovibrator model of the doubly excited states gives a deeper physical insight into the mechanism of the double-electron excitation.

PACS number(s): 34.50.Fa, 31.50.+w, 31.20.Tz

I. INTRODUCTION

In our previous paper [1], we investigated double-electron excitation process to understand the role of the electron-electron correlation in ion-atom collisions, that is,



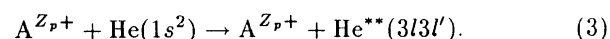
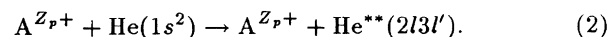
where we treated a proton, an antiproton, and a C^{6+} ion at 1–10 MeV/u impact energies as the projectile (A^{Z_p+}).

This study was motivated by an experiment at CERN on double ionization of He atom at a few MeV/u impact energy by proton and antiproton impact by Andersen *et al.* [2]. In their experiment, it has been found that the cross section by the antiproton impact is about two times as large as that by the proton impact in spite of the high impact energy used, while both single-ionization cross sections are almost equal to one another. Recent studies on the double ionization [3, 4] have suggested the importance of the electron correlation. Therefore we studied process (1) because this process is the simplest one in which the correlation effect is expected to play a decisive role.

The difference between the double-electron excitation cross section by proton impact and that by an-

tiproton impact was found to be much smaller than that corresponding to double-ionization processes. However we have found that we cannot ignore second-order processes except for the $(1s^2)^1S^e$ – $(2s2p)^1P^o$ excitation where the first-order direct excitation dominates. After assessing the importance of intermediate states for each second-order process, we have seen that dipole transitions ($\Delta L=1$) are likely to take place in these collision processes as is expected. In particular, the $^1P^o$ plays an important role as an intermediate state in the second-order excitation process to the doubly excited $^1S^e$, and $^1D^e$ state. Further we have found that the doubly excited $2s2p^1P^o$ state plays the most important role as an intermediate state.

In this paper, we investigate double-electron excitation processes to the higher doubly excited states, that is,



Here we treated the proton, and the antiproton at 1.5 MeV/u impact energy as the projectile (A^{Z_p+}). The purpose of the present paper is to understand the role of the correlation effects and the mechanism in these colli-

sion processes, and, in particular, to investigate whether or not the same mechanism as found in process (1) operates in processes (2) and (3).

II. SUMMARY OF THEORETICAL TREATMENT

We employ the same theoretical framework as that used in Ref. [1]. Here we describe it briefly. Namely, we use close-coupling method with semiclassical impact-parameter method to calculate the double-electron excitation cross sections. We neglect the charge-transfer channels in these processes because charge-transfer cross sections are quite small in comparison with excitation

cross sections in the high incident energies studied here. Therefore for processes (2) and (3) we expand the total wave function in terms of the He wave functions centered on the He^{2+} nucleus. We generate the He wave functions employing the hyperspherical-coordinate method which allows us to describe the electron-electron correlation accurately. Lifetimes for the autoionizing states [5–7] are short in comparison with collision times at their energy range. Recent study on the $(2s)^2$ double excitation of He [8] suggests the possible effect of the continuum as intermediate states. However, in this study we also ignore the coupling with the continuum in order to investigate the mechanism of the higher excitation within our theoretical

TABLE I. Doubly excited states included in the 85-state calculation of the cross sections. The first column gives a set of the quantum numbers for the main electronic configuration based on independent-particle model (IPM), the second column shows a set of correlation quantum numbers $[N(K, T)^A n]$, the third column gives the values of the binding energies (BE) (in the unit of Rydberg) of the doubly excited states calculated from our hyperspherical wave functions, and the fourth column gives the values of the binding energies based on an elaborate calculation [6, 9]. The set (a) of the states are adopted in the 73-state CC calculation and the sets (a) and (b) are included in the 85-state CC calculation.

IPM	$N(K, T)^A n$	BE (Ry)	
		Present	Previous
(a)			
$1s1s^1 S^e$	$[1(0, 0)^+ 1]^1 S^e$	-5.791	
$1s2s^1 S^e$	$[1(0, 0)^+ 2]^1 S^e$	-4.280	
$1s3s^1 S^e$	$[1(0, 0)^+ 3]^1 S^e$	-4.119	
$1s4s^1 S^e$	$[1(0, 0)^+ 4]^1 S^e$	-4.066	
$1s5s^1 S^e$	$[1(0, 0)^+ 5]^1 S^e$	-4.042	
$2s2s^1 S^e$	$[2(1, 0)^+ 2]^1 S^e$	-1.544	-1.556*
$2s3s^1 S^e$	$[2(1, 0)^+ 3]^1 S^e$	-1.169	-1.180*
$2s4s^1 S^e$	$[2(1, 0)^+ 4]^1 S^e$	-1.084	
$2p2p^1 S^e$	$[2(-1, 0)^+ 2]^1 S^e$	-1.211	-1.240*
$2p3p^1 S^e$	$[2(-1, 0)^+ 3]^1 S^e$	-1.088	-1.096*
$2p4p^1 S^e$	$[2(-1, 0)^+ 4]^1 S^e$	-1.051	
$3s3s^1 S^e$	$[3(2, 0)^+ 3]^1 S^e$	-0.7058	-0.7071†
$3p3p^1 S^e$	$[3(0, 0)^+ 3]^1 S^e$	-0.6147	-0.6349†
$3d3d^1 S^e$	$[3(-2, 0)^+ 3]^1 S^e$	-0.5102	-0.5148†
$1s2p^1 P^o$	$[1(0, 0)^0 2]^1 P^o$	-4.243	
$1s3p^1 P^o$	$[1(0, 0)^0 3]^1 P^o$	-4.108	
$1s4p^1 P^o$	$[1(0, 0)^0 4]^1 P^o$	-4.061	
$2s2p^1 P^o$	$[2(0, 1)^+ 2]^1 P^o$	-1.389	-1.386*
$(2s3p + 3s2p)^1 P^o$	$[2(0, 1)^+ 3]^1 P^o$	-1.122	-1.128*
$(2s4p + 4s2p)^1 P^o$	$[2(0, 1)^+ 4]^1 P^o$	-1.066	
$3s3p^1 P^o$	$[3(1, 1)^+ 3]^1 P^o$	-0.6754	-0.6713*
$3p3d^1 P^o$	$[3(-1, 1)^+ 3]^1 P^o$	-0.5576	
$1s3d^1 D^e$	$[1(0, 0)^0 3]^1 D^e$	-4.111	
$2p2p^1 D^e$	$[2(1, 0)^+ 2]^1 D^e$	-1.399	
$2p3p^1 D^e$	$[2(1, 0)^+ 3]^1 D^e$	-1.129	
$2s3d^1 D^e$	$[2(0, 1)^0 3]^1 D^e$	-1.112	
$3p3p^1 D^e$	$[3(2, 0)^+ 3]^1 D^e$	-0.6913	
$3s3d^1 D^e$	$[3(0, 2)^+ 3]^1 D^e$	-0.6218	
$3d3d^1 D^e$	$[3(0, 0)^+ 3]^1 D^e$	-0.5651	
(b)			
$(2s3p - 3s2p)^1 P^o$	$[2(1, 0)^- 3]^1 P^o$	-1.187	-1.194*
$(2s4p - 4s2p)^1 P^o$	$[2(1, 0)^- 4]^1 P^o$	-1.089	
$2p3d^1 P^o$	$[2(-1, 0)^0 3]^1 P^o$	-1.090	-1.094*
$2p4d^1 P^o$	$[2(-1, 0)^0 4]^1 P^o$	-1.053	

*Reference [6].

†Reference [9].

framework as employed in our previous work [1].

Table I lists the 85 states included in our close-coupling (CC) calculation. At first, we have included 73 states in the close-coupling calculation listed in Table I. To test the convergence of the cross sections with respect to the numbers of the states included by adding some possibly important states such as the $(2s3p-3s2p)^1P^o$, and $2p3d^1P^o$ states, we have found that the set of the $(2l, 3l')$ cross sections by the 85-state CC calculation converges within a few percent. The set of the cross sections of the $(3l, 3l')$ excitation of the 73-state CC calculation agree with those of the 85-state CC calculation within some 10% except for the cases of the excitation to the $3s3s^1S^e$ and $3d3d^1D^e$ states where the difference between the two sets of cross sections is some 20%. In the latter cases, the second-order processes are seen to be more important. Hence we consider that the 85-state results are more reliable because we have added some important intermediate states in the 85-state CC calculation to the set of the 73 states. Here we have confirmed that the set of the 21-state CC cross sections to the $(2l, 2l')$ manifold [1] is in agreement with that corresponding to the $(2l, 2l')$ excitation of the present 85-state CC results within 5%. In the 85-state CC calculation, we have ignored some potential coupling elements, for example, that between the $(2s3p-3s2p)^1P^o$ state and the $2s3d^1D^e$ state, which are found to have little influence on the excitation to the $2l3l'$ and $3l3l'$ manifolds.

Table I gives the values of the binding energies of doubly excited states calculated from our hyperspherical wave functions and the values of the binding energies based on the elaborate calculation available at present [6, 9]. Comparison of our calculated binding energies with the latter enables one to assess the accuracy of our hyperspherical wave functions employed in the present 85-state CC calculation.

Table I also lists the labelings $[N(K, T)^A n]$ based on the correlation quantum number K, T, A [10, 11] for the states included in the CC calculation. Here N (n) is the principal quantum number of an inner (outer) electron. The quantum numbers K and T originate from the group-theoretical approach by Sinanoğlu and Herrick [12] and describe angular correlation of the two electrons, on the other hand the quantum number A introduced by Lin describes the radial correlation of the two atomic electrons. This quantum number is set equal to $+$ ($-$) if the angular channel function has antinode (node) at $\alpha = \pi/4$ where α is a hyperangle defined by $\alpha = \tan^{-1}(r_2/r_1)$. Other channels are assigned to $A = 0$ where their channel functions do not have substantial amplitudes around $\alpha = \pi/4$ for almost all values of the hyperradius R ($= \sqrt{r_1^2 + r_2^2}$) but reside instead at $\alpha = 0$ or $\pi/2$. All these quantum numbers are approximate ones because the two-electron Schrödinger equation is only approximately separable into the collective motions of the two atomic electrons.

In the present paper, we will employ the 85-state CC cross sections in later discussion and make physical interpretation of the results obtained based on the labelings by the set of the correlation quantum numbers and on

the rovibrator model of the doubly excited states to get a deeper physical insight into the excitation mechanism.

III. RESULTS AND DISCUSSION

A. $2l3l'$ cross sections

Table II gives the excitation cross sections from the ground state to the doubly excited intershell $2l3l'$ states at 1.5 MeV/u by the proton and antiproton impact. The cross sections evaluated by the first-Born approximation are given in column (2) of the same table. The magnitude of the cross sections is about one-fifth as large as that to the $2l2l'$ state. The cross sections by the proton impact $\sigma(p)$ are larger than those by the antiproton impact $\sigma(\bar{p})$ except for the processes to the doubly excited $(2s3p+3s2p)^1P^o$ and $(2s3p-3s2p)^1P^o$ states. In the cases of these two processes, each $\sigma(p)$ is almost equal to $\sigma(\bar{p})$. The difference between $\sigma(\bar{p})$ and $\sigma(p)$ is almost equal to that in the cases of the double-electron $2l2l'$ excitation, and is much smaller than that in the case of the double ionization [2]. However we find that we cannot ignore higher-order processes by comparing between the cross sections calculated with the close-coupling method and those with the first Born approximation similarly to the case of the doubly excited $2l2l'$ states [see column (1) and (2) in Table II]. As we have already seen for process (1), it is unlikely that n th higher-order processes with $n > 2$ do not play an important role in processes (2) and (3) by the proton and antiproton impact in the MeV energy region.

We assess the importance of intermediate states for each excitation process by evaluating the cross section with a particular state excluded [columns (3)–(6) in Table II]. For excitation to the $2s3s^1S^e$ and $2p3p^1S^e$ states, one finds that an important intermediate state is the $(2s3p+3s2p)^1P^o$ state. Here the $(2s3p+3s2p)^1P^o$ state is found to play the same crucial role as the $2s2p^1P^o$ state in the case of the process to the $2l2l'^1S^e$ states. For excitation to the $(2s3p+3s2p)^1P^o$ and $(2s3p-3s2p)^1P^o$ states, the first-order processes dominates similarly to the process to the $2s2p^1P^o$ state (compare the second column with the other ones in Table II). However the second-order processes exist in the process to the $2p3d^1P^o$ state. We also find that the important intermediate state is the $1s2p^1P^o$ state. For the process to the $2p3p^1D^e$ and $2s3d^1D^e$ states, second-order processes dominate similarly to the process to the $2p2p^1D^e$ state. The important intermediate states are the $1s3p^1P^o$, and $(2s3p+3s2p)^1P^o$ states for the $2p3p^1D^e$ excitation, and the $1s3p^1P^o$, $2s2p^1P^o$ and $(2s3p+3s2p)^1P^o$ states for the $2s3d^1D^e$ excitation. In these studies, one sees either that first-order mechanism dominates such as in the $2s2p^1P^o$ excitation or that the second-order mechanism prevails over the first one as typically seen in the $2p3p^1D^e$ excitation. This gives rise to a smaller interference effect which gives the small difference between $\sigma(p)$ and $\sigma(\bar{p})$ as was seen in the $(2l, 2l')$ excitation.

Generally speaking, the mechanism of the excitation processes to the doubly excited $2l3l'$ states is almost the

TABLE II. Double-electron excitation cross sections (in units of 10^{-20} cm^2) of He atoms at 1.5 MeV/u impact energies by proton and antiproton impact. Column (1) lists the cross sections calculated with the 85 states for the excitation included in the close-coupling method. Column (2) gives ones by the first-Born approximation, and columns (3)–(6) give the calculated cross sections with the following state excluded from the set of the 85 states. (3) $1s2p^1P^\circ$, (4) $1s3p^1P^\circ$, (5) $2s2p^1P^\circ$, and (6) $(2s3p + 3s2p)^1P^\circ$.

Final states	Cross section (10^{-20} cm^2)					
	(1)	(2)	(3)	(4)	(5)	(6)
Proton impact						
$2s3s^1S^e$	0.0955	0.0827	0.0957	0.0938	0.0984	0.0827
$2p3p^1S^e$	0.0234	0.0132	0.0231	0.0202	0.0181	0.0148
$(2s3p + 3s2p)^1P^\circ$	1.35	1.39	1.36	1.34	1.33	
$(2s3p-3s2p)^1P^\circ$	0.0264	0.0292	0.0315	0.0260	0.0267	0.0196
$2p3d^1P^\circ$	0.00236	0.00197	0.00315	0.00227	0.00252	0.00140
$2p3p^1D^e$	0.0278	0.00279	0.0335	0.00622	0.0263	0.0196
$2s3d^1D^e$	0.0102	0.00593	0.00947	0.0180	0.00864	0.0230
Antiproton impact						
$2s3s^1S^e$	0.0791	0.0827	0.0793	0.0800	0.0793	0.0840
$2p3p^1S^e$	0.0202	0.0132	0.0193	0.0134	0.0173	0.0163
$(2s3p + 3s2p)^1P^\circ$	1.37	1.39	1.36	1.39	1.36	
$(2s3p-3s2p)^1P^\circ$	0.0331	0.0292	0.0301	0.0374	0.0352	0.0317
$2p3d^1P^\circ$	0.00200	0.00197	0.00213	0.00267	0.00186	0.00233
$2p3p^1D^e$	0.0275	0.00279	0.0298	0.00938	0.0275	0.0172
$2s3d^1D^e$	0.00758	0.00593	0.00622	0.0147	0.0140	0.0139

same as that of the processes to the doubly excited $2l2l'$ states except that the cross sections are about one-fifth as large as those corresponding to the $(2l2l')$ excitation. The decrease of the magnitude of the cross sections is attributable to the smaller overlap of the $(2l3l')$ final-state wave functions with the ground-state wave function in comparison with that of the $(2l2l')$ ones. In these collision processes, the $^1P^\circ$ states play an important role as a decisive intermediate state in the excitation process to the doubly excited $^1S^e$, and $^1D^e$ state.

B. $3l3l'$ cross sections

Table III shows the cross sections to the $3l3l'$ states at 1.5 MeV/u. For the processes to the $3l3l'$ states, the difference between $\sigma(p)$ and $\sigma(\bar{p})$ is much smaller than that corresponding to double-ionization processes except for the $3p3p^1S^e$ excitation which will be discussed later. The small overlap of the ground-state wave function with the $3l3l'$ excited wave functions strongly suppresses the first-order amplitude for the two-electron excitation and the second-order mechanisms dominate. This makes the interference effect rather small, which may also explain the small difference between $\sigma(p)$ and $\sigma(\bar{p})$.

We have also assessed the importance of each intermediate state in this process in the similar manner as in the case of the $(2l, 3l')$ excitations [columns (3)–(10) in Table III]. The ratio of the second-order process to the first-order one is much larger than that in the case of the process to the $2l2l'$ or $2l3l'$ state (compare the second

column with the other set of cross sections in Table III). The $(3s3p)^1P^\circ$ states which are strongly coupled with the other $3l3l'$ states do not play a crucial role. This is in a sharp contrast with the excitation to the $(2l, 2l')$ and $(2l, 3l')$ manifolds. As a result, there exist more states which are involved as relatively important intermediate states in these excitation processes than those corresponding to the double-electron $2l2l'$ or $2l3l'$ excitation processes.

For the process to the $(3l3l)^1S^e$ states, we find that the $1s2s^1S^e$, $1s3s^1S^e$, $1s2p^1P^\circ$, $1s3p^1P^\circ$, and $2s2p^1P^\circ$ states are important as intermediate states and a group of these intermediate states is different from that of the process to the $2l2l'$ or $2l3l'$ states. Namely, the singly excited $^1S^e$ states are important, while the $(3l3l')^1P^\circ$ states are not. Either the $1s2s^1S^e$ or $1s3s^1S^e$ state causes large difference to the set of the cross sections when we exclude these two states from the expansion separately. However when two states are simultaneously excluded from the set of the 85 states, the resulting cross sections (compare the first column with the fifth column of Table III) remain almost the same as those of the 85-state CC calculation. This is considered to arise from the destructive interference effect between the process from the $1s2s^1S^e$ state to the $3l3l^1S^e$ state and that from the $1s3s^1S^e$ to the $(3l3l)^1S^e$ state. Furthermore, this trend is more clearly seen when we exclude all singly excited $^1S^e$ states.

As to the large difference of the $3p3p^1S^e$ excitation between $\sigma(p)$ and $\sigma(\bar{p})$, a possible explanation is that there are several relatively important intermediate states as seen in Table III, which may make the second-order am-

TABLE III. Double-electron excitation cross sections (in units of 10^{-23} cm²) of He atoms at 1.5MeV/u impact energies by proton and antiproton impacts. Column (1) lists sets of the cross sections calculated with the 85 states included in the close-coupling method, column (2) gives ones by the first-Born approximation, and columns (3)–(8) gives the calculated cross sections with the following state excluded from the set of 85 states (3) $1s2s^1S^e$, (4) $1s3s^1S^e$, (5) $1s2s^1S^e$ and $1s3s^1S^e$ states, (6) $1s3p^1P^o$, (7) $2s2p^1P^o$, and (8) $(2s3p + 3s2p)^1P^o$.

Final states	Cross section (10^{-23} cm ²)							
	(1)	(2)	(3)	(4)	(5)	(6)	(7)	(8)
Proton impact								
$3s3s^1S^e$	0.055	0.0015	0.29	0.42	0.045	0.20	0.11	0.059
$3p3p^1S^e$	0.091	0.023	0.34	0.24	0.13	0.12	0.19	0.044
$3d3d^1S^e$	0.016	0.013	0.042	0.069	0.018	0.059	0.021	0.048
$3s3p^1P^o$	0.72	0.49	1.1	1.5	0.60	1.1	1.8	0.79
$3p3d^1P^o$	0.54	0.44	0.96	0.78	0.57	0.79	0.81	0.52
$3p3p^1D^e$	0.99	0.17	1.2	0.97	1.1	4.1	0.50	1.4
$3s3d^1D^e$	0.13	0.0029	0.14	0.15	0.13	0.99	2.1	0.83
$3d3d^1D^e$	0.32	0.017	0.35	0.32	0.34	1.0	0.61	0.38
Antiproton impact								
$3s3s^1S^e$	0.049	0.0015	0.33	0.39	0.043	0.24	0.15	0.028
$3p3p^1S^e$	0.030	0.023	0.19	0.14	0.042	0.14	0.080	0.032
$3d3d^1S^e$	0.018	0.013	0.047	0.053	0.020	0.11	0.027	0.021
$3s3p^1P^o$	0.65	0.49	0.95	1.8	0.42	0.63	1.5	0.76
$3p3d^1P^o$	0.55	0.44	0.84	0.99	0.51	0.71	0.67	0.71
$3p3p^1D^e$	0.93	0.17	0.86	1.0	0.89	4.0	0.83	1.1
$3s3d^1D^e$	0.18	0.0029	0.17	0.22	0.16	1.0	2.2	0.59
$3d3d^1D^e$	0.28	0.017	0.30	0.28	0.28	0.91	0.58	0.30

plitude smaller by cancellation and comparable with the small first-order amplitude. This may enhance the difference between $\sigma(p)$ and $\sigma(\bar{p})$ though the absolute magnitude of the $3p3p^1S^e$ excitation cross section is rather small.

For the excitation process to the $(3l3l')^1P^o$ states, there exist the second-order processes. However the ratio of the second-order process to the first-order process is much smaller than that in the case of the process to the $(3l3l)^1S^e$ and $(3l3l')^1D^e$ states. We regard the $1s2s^1S^e$, $1s3s^1S^e$, $1s2p^1P^o$, $1s3p^1P^o$, and $2s2p^1P^o$ states as important intermediate states. For the $(3l3l')^1P^o$ excitation processes, we also find that the effects of the $1s2s^1S^e$ and $1s3s^1S^e$ states as intermediate states seem to cancel out because of destructive interference (compare the first column with the fifth column of Table III).

For the excitation process to the $3s3p^1P^o$ state, the doubly excited $2s2p^1P^o$ and $(2s3p + 3s2p)^1P^o$ states play a more important role as intermediate states than the singly excited $^1P^o$ states. For the process to the $3p3d^1P^o$ state, the contribution from the singly and doubly excited states becomes comparable.

For the process to the $(3l3l')^1D^e$ states, the ratio of the second-order process to the first-order process is larger than that in the case of the process to the $(3l3l)^1S^e$ and $(3l3l')^1P^o$ states. We regard the $1s2p^1P^o$, $1s3p^1P^o$, $2s2p^1P^o$, and $(2s3p + 3s2p)^1P^o$ states as important intermediate states. For the excitation to the $3p3p^1D^e$ and $3d3d^1D^e$ states, the singly excited $^1P^o$ states play more

significant roles as the intermediate state than the doubly excited $(2snp + ns2p)^1P^o$ states. On the other hand, for the excitation to the $3s3d^1D^e$ state, the doubly excited $(2snp + ns2p)^1P^o$ states play more significant roles as the intermediate state.

C. Physical interpretation of the results based on the rovibrator model of the doubly excited states

Matsuzawa and his co-workers [13–16] investigated collisional behaviors of He atoms in the strongly correlated doubly excited state by charged-particle impact. They found a set of propensity rules for the excitation processes of He by charged-particle impact. According to the rovibrational interpretation of collective modes [17], He atoms in strongly correlated states are viewed as a flexible “e-He²⁺-e” triatomic linear molecule. These rules indicate that the He atoms in the correlated doubly excited states tend to conserve their internal states as a flexible “e-He²⁺-e” triatomic linear molecule when they interact with charged particles perturbatively, i.e., radial propensity rule

$$\Delta A = 0 \quad (4)$$

and angular propensity rules

$$\Delta v = 0 \quad \text{and} \quad \Delta T = 0. \quad (5)$$

Here, according to the rovibrator model, $v (= N - K - 1)$

corresponds to the quantum number of the doubly degenerate bending vibrational modes and T is reinterpreted as the vibrational angular momentum around the mean molecular axis of the "e-He²⁺-e" molecule. The latter propensity rules lead to the following rule:

$$\Delta n_2 = 0, \quad (6)$$

where $n_2 [= (v - T)/2]$ is the radial bending quantum number. This is interpreted as a result of the isomorphism of the charge-density plots of the channel wave functions between the initial excited states and the final ones. This means that there is no change of the nodal structures between the initial and final-state channel functions and guarantees the largest overlap between the initial and final-state wave functions. However, for the singlet-singlet optically allowed excitation with $|\Delta L| = 1$, the radial propensity rule (4) is incompatible with the angular ones (5) because the two atomic electrons obey Fermi statistics, i.e., because there exists the following relation between A and T :

$$A = \pi(-1)^{S+T} \quad (7)$$

arising from the Pauli exclusion principle [18]. For the initial state with $A = +$, the radial propensity rule prevails over the angular ones and the latter is modified into

$$\Delta v = \Delta T = 1 \quad (8)$$

while the propensity rule (6) remain unchanged. It should be noted that a set of the propensity rules (4), (8) [instead of (5)] and (6) also applies to photoabsorption of He.

For the processes to the $(2l, 3l')$ manifold in Sec. III A (see Table II and the discussion given in Sec. III A), the first-order process dominates in the excitation process from the ground $1s1s^1S^e \{[1(0,0)+1]^1S^e, (v=0)\}$ state to the $(2s3p + 3s2p)^1P^o \{[2(0,1)+3]^1P^o, (v=1)\}$ state. This is consistent with the set of the propensity rules (4), (8) [instead of (5)], and (6). Namely, the probability flux is at first transferred to the $(2s3p + 3s2p)^1P^o \{[2(0,1)+3]^1P^o, (v=1)\}$ state. Then it is distributed over the other doubly excited states of the $(2l, 3l')$ manifold in the second step. However, in the second steps of the second-order processes, there is no case which is consistent with the propensity rules. This arises from the fact that there is no final state available within the $(2l, 3l')$ manifold that the above-propensity rules specify because of the cutoff of the quantum number K (or v) and T .

For the excitation to the $(3l, 3l')$ manifold (see Table III and the discussion given in Sec. III B), the first-order process to the $3s3p^1P^o \{[3(1,1)+3]^1P^o, (v=1)\}$ state is not so dominant as in the cases of excitation to the $(2l, 2l')$ and $(2l, 3l')$ manifolds which is consistent with the set of the propensity rules, i.e., (4), (8), and (6). On the other hand, there exist the dominant second-order processes via the $2s2p^1P^o \{[2(0,1)+2]^1P^o, (v=1)\}$ and the $(2s3p + 3s2p)^1P^o \{[2(0,1)+3]^1P^o, (v=1)\}$ states though there are other important routes to the $(3l, 3l')$ manifold via the singly excited states such as $1sn s^1S^e$ and $1snp^1P^o$ states. This is in a sharp contrast to ex-

citation to the $(2l, 2l')$ and $(2l, 3l')$ manifolds. It is attributable to the fact that the $(3s3p)^1P^o \{[3(1,1)+3]^1P^o, (v=1)\}$ -state wave function has a quite small overlap directly with the ground- $1s1s^1S^e \{[1(0,0)+1]^1S^e, (v=0)\}$ -state wave function because the mean size of the He atom in the excited $[3(1,1)+3]^1P^o$ state is quite different from that in the ground state. Therefore the $2s2p^1P^o \{[2(0,1)+2]^1P^o, (v=1)\}$ and $(2s3p + 3s2p)^1P^o \{[2(0,1)+3]^1P^o, (v=1)\}$ states play decisive roles in the excitation processes to the $(3l, 3l')$ manifold. This can also explain the relative importance of the second-order processes (a ladder-climbing mechanism) to the first-order ones (a direct excitation mechanism) seen in the excitation to the $(3l, 3l')$ manifold.

We can easily visualize how the two strongly correlated atomic electrons behave during the second-order excitation processes such as the successive transitions $1s1s^1S^e \{[1(0,0)+1]^1S^e, (v=0)\} \rightarrow 2s2p^1P^o \{[2(0,1)+2]^1P^o, (v=1)\} \rightarrow 3s3p^1P^o \{[3(1,1)+3]^1P^o, (v=1)\}$. In this case the first step is consistent with the set of the propensity rules (4), (8) and (6) with $\Delta L = 1$. The He atom as the flexible "e-He²⁺-e" triatomic linear molecule becomes vibrationally excited in the doubly degenerate bending vibrational modes and rotationally excited around the mean molecular axis stretching its size. The second step corresponds with the set of the propensity rules, (4), (5), and (6) and the He atom simply stretches its size conserving its internal state as the flexible linear molecule consistently with the set of the propensity rules. For other processes, one can easily give a visual illustration of the behaviors of the correlated motion for two atomic electrons based on the labelings by the set of correlation quantum numbers given in Table I.

IV. SUMMARY AND CONCLUSIONS

We have theoretically investigated the double-electron excitation of He to the $2l3l'$ and $3l3l'$ states by the proton and antiproton impact using the hyperspherical wave functions for the description of the electron-electron correlation. At 1.5 MeV/u, we have found that the difference for the double-electron excitation processes by the proton and antiproton impact is much smaller than that corresponding to the double-ionization processes except for the process to the $3p3p^1S^e$ state. The first-order processes dominates in the excitation process to the $(2s3p \pm 3s2p)^1P^o$ states by the proton and antiproton impact. In the excitation process to the $2s3d^1D^e$ and $2p3p^1D^e$ states, the second-order process dominates. This situation makes the interference between the first- and second-order mechanisms small, which can explain the small difference between $\sigma(p)$ and $\sigma(\bar{p})$ though, in the excitation to the $2p3d^1P^o$, $2s3s^1S^e$, and $2p3p^1S^e$ states, the first- and second-order processes give more comparable contribution to these processes, which gives larger difference between $\sigma(p)$ and $\sigma(\bar{p})$. In the processes to the $2l3l'$ state, the doubly excited $(2s3p + 3s2p)^1P^o$ state plays an essential role as an intermediate state.

In the processes to the $3l3l'$ states, the second-order processes dominate, which also explain the small difference between $\sigma(p)$ and $\sigma(\bar{p})$ because of the small over-

lap of the ground-state wave function with the $3l, 3l'$ excited wave function. In the processes to the $(3l, 3l')^1S^e$ and $(3l, 3l')^1P^o$ states, the singly excited $^1S^e$ and $^1P^o$ states play important role as intermediate states. However, when the all singly excited states are simultaneously excluded, the resulting role of these intermediate states is found to become much weaker. In the process to the $(3l, 3l')^1D^e$ states, the $1s2p^1P^o$, $1s3p^1P^o$, $2s2p^1P^o$, and $(2s3p + 3s2p)^1P^o$ states play important roles as intermediate states. The difference between the excitation mechanisms to the $(2l, 2l')$ and $(2l, 3l')$ manifolds and that to the $(3l, 3l')$ manifold, i.e., the relative importance of the ladder-climbing mechanism in the excitation to the $(3l, 3l')$ manifolds, is considered to arise from the smaller overlap of the $(3l, 3l')$ wave functions with the ground state one. These findings result from the difference of the mean sizes of the He atom in the final doubly excited states. The physical interpretation based on the rovibrator models gives a deeper physical insight into the excitation mechanisms, in particular, into the difference between the mechanism into the excitation to the $(2l, 2l')$ and $(2l, 3l')$ manifolds and that to the $(3l, 3l')$ manifold.

This difference suggests that the excitation mechanism

to higher $(nl, n'l')$ manifolds with $n \geq 3$, $n' \geq 4$ is similar to that to the $(3l, 3l')$ manifold because of the quite small overlap of their wave functions with the ground-state wave function except that there exists no intermediate doubly excited state corresponding to the $(2s2p)^1P^o$ and $(2s3p + 3s2p)^1P^o$ states. Finally, a study on the effect of the continuum in the two-electron excitation processes is in progress using the discretization method.

ACKNOWLEDGMENTS

We wish to thank S. Watanabe and N. Koyama for their useful discussion. Two of us (M.M. and M.K.) gratefully acknowledge the support from the international cooperative research program between the National Science Foundation and the Japan Society for the Promotion of Science. One of us (M.K.) also acknowledges the support from the U.S. DOE office of Health and Environment Research under Contract No. W31-109-Eng-38. Numerical computations were carried out in part at the Computer Center, Institute for Molecular Science, Okazaki National Research Institutes.

-
- [1] K. Moribayashi, K. Hino, M. Matsuzawa, and M. Kimura, *Phys. Rev. A* **44**, 7234 (1991).
 - [2] L. H. Andersen, P. Hvelplund, H. Knudsen, S. P. Møller, K. Elsener, K.-G. Rensfelt, and E. Uggerhøj, *Phys. Rev. Lett.* **57**, 2147 (1986).
 - [3] J. F. Reading and A. L. Ford, *Phys. Rev. Lett.* **58**, 543 (1987); *J. Phys. B* **20**, 3747 (1987).
 - [4] A. L. Ford and J. F. Reading, *J. Phys. B* **21**, L685 (1988).
 - [5] P. G. Burke, *Adv. At. Mol. Phys.* **4**, 173 (1968).
 - [6] Y. K. Ho, *J. Phys. B* **12**, 387 (1979).
 - [7] A. K. Bhatia and A. Temkin, *Phys. Rev. A* **11**, 2018 (1975).
 - [8] T. G. Winter, *Phys. Rev. A* **43**, 4727 (1991).
 - [9] Y. K. Ho, *Phys. Rev. A* **23**, 2137 (1981).
 - [10] C. D. Lin, *Phys. Rev. A* **29**, 1019 (1984).
 - [11] C. D. Lin, *Adv. At. Mol. Phys.* **22**, 77 (1986).
 - [12] O. Sinanoğlu and D. R. Herrick, *J. Chem. Phys.* **62**, 886 (1975).
 - [13] M. Matsuzawa, T. Motoyama, H. Fukuda, and N. Koyama, *Phys. Rev. A* **34**, 1793 (1986).
 - [14] T. Motoyama, N. Koyama, and M. Matsuzawa, *Phys. Rev. A* **38**, 670 (1988).
 - [15] M. Matsuzawa, T. Atsumi, and N. Koyama, *Phys. Rev. A* **41**, 3596 (1990).
 - [16] T. Atsumi, T. Ishihara, N. Koyama, and M. Matsuzawa, *Phys. Rev. A* **42**, 6391 (1990).
 - [17] M. E. Kellman and D. R. Herrick, *Phys. Rev. A* **22**, 1536 (1980).
 - [18] S. Watanabe and C. D. Lin, *Phys. Rev. A* **34**, 823 (1986).